Proceedings of the 16th Virtual International Meeting on Fully 3D Image Reconstruction in Radiology and Nuclear Medicine

Editors: Georg Schramm, Ahmadreza Rezaei, Kris Thielemans and Johan Nuyts

2D study of a joint reconstruction algorithm for limited angle PET geometries

Marina Vergara[1,2], Ahmadreza Rezaei[1], Maria Jose Rodriguez-Alvarez[2], Jose Maria Benlloch Baviera[2], and Johan Nuyts[1]

[1]Department of Imaging and Pathology, Division of Nuclear Medicine, KU Leuven, Belgium
[2]Instituto de Instrumentacion para Imagen Molecular Centro Mixto CSIC—Universitat Politecnica de València, Valencia, Spain

Abstract Recently, a wide interest on organ-dedicated PET systems has been shown. Some of those systems present geometries that produce an incomplete sampling of the tomographic data due to limited angular coverage and/or truncation, which lead to artifacts on the reconstructed image. Moreover, they are often designed as stand-alone systems, which implies the absence of anatomical information to estimate the attenuation factors. In this work, we propose a joint reconstruction algorithm for estimating the activity and the attenuation factors on a limited angle PET system with time-of-flight capabilities. This algorithm is based on MLACF and uses literature linear attenuation coefficients in a known tissue-class region to obtain an absolute quantification. We evaluate the algorithm through simple 2D simulations for different TOF resolutions and angular coverage. The results show that with good TOF resolution quantitative PET imaging can be achieved even with aggressive angular limitation.

1 Introduction

In recent years, organ-dedicated PET (positron emission tomography) systems have been proposed as an alternative to the whole-body scanner. These systems are focused on being less expensive, requiring less space and/or providing easier patient access, having higher resolution and/or better sensitivity [1]. They are typically stand-alone systems, which means the absence of supplementary CT or MR systems that could be used to provide the attenuation image. Many such systems use a geometry that can lead to limited angular coverage and, therefore, the acquisition of incomplete tomographic data. Because the reconstruction from these data does not have a unique solution, the reconstructed images usually suffer from artifacts. It has been shown that in PET, the availability of TOF (time-of-flight) information reduces these limited angle artefacts [2, 3].

When data are provided with TOF information, joint reconstruction algorithms can be used to estimate the attenuation sinogram from the emission data up to a global constant [4] for all the LORs where activity is present, so long as the spread of the tracer is wider than the TOF resolution. This constant can be determined if prior knowledge about attenuation (or activity) values is available [5–8].

In this work we consider the problem of jointly reconstructing the activity image and the attenuation sinogram from TOF-PET data suffering from limited angular coverage or truncation. We propose an approach based on the MLACF algorithm of [9]. For limited angle data, it is not guaranteed that all sinogram pixels are affected by the same constant, but below we show that in many cases this will be the case. To determine the value of the constant, the attenuation image is reconstructed from the estimated attenuation coefficients. The problem is only studied in 2D. As shown below, the results indicate that for PET with high TOF resolution, quantitative image reconstruction can be achieved even for systems providing very limited angular coverage and severe truncation.

The work presented here has also been submitted to IEEE TRPMS [10]

2 Materials and Methods

2.1 System design

In order to examine the effect of limited angular coverage in TOF-PET image reconstruction, we use a 2D simulation of a partial arc of a circular PET. We consider limited angle effects similar to those seen by a pair of flat panels of size W, separated by distance D, by setting to zero the sensitivity value of all the LORs that are not seen by both flat panels (LOR 1 and 3 in figure 1).

2.2 Joint reconstruction

In order to exploit the TOF information in the joint estimation of activity and attenuation process, Maximum Likelihood estimation of the activity and the Attenuation Correction Factors (MLACF) [9] is applied.

In TOF PET, the expected count $\bar{y}_{it}$ for a certain line of response (LOR) i and TOF-bin t can be written as:

$$\bar{y}_{it} = a_i p_{it} + r_{it} \quad \text{with} \quad p_{it} = \sum_j c_{ijt}\lambda_j \tag{1}$$

where p_{it} is the unattenuated TOF projection of the activity image λ_i for LOR i in TOF-bin t, a_i is the total linear attenuation coefficient along the LOR i, c_{ijt} is the sensitivity of the measurement bin (i,t) for activity in voxel j in the absence of the attenuation and r_{it} is an additive contribution made by randoms and/or scatter.

Then the MLACF algorithm [9] is given by:

$$\lambda_j^{(n+1)} = \frac{\lambda_j^{(n)}}{\sum_i c_{ij} a_i^{(m+1)}} \sum_{it} c_{ijt} a_i^{(m+1)} \frac{y_{it}}{\sum_k c_{ikt} a_i^{(m+1)} \lambda_k^{(n)} + r_{it}}, \tag{2}$$

$$a_i^{(m+1)} = a_i^{(m)} \sum_t \frac{p_{it}^{(n)}}{p_i^{(n)}} \frac{y_{it}}{a_i^{(m)} p_{it}^{(n)} + r_{it}}. \quad (3)$$

where n and m denote the iteration numbers for the activity and the attenuation correction factors (ACFs), respectively, and $p_i^{(n)} = \sum_t p_{it}^{(n)}$. Also for other TOF-dependent variables, we will drop the TOF-index to denote summation over the TOF-bins.

TOF data determine the attenuation sinogram up to a constant, which correspond to a multiplicative factor in the activity image. To obtain it, we propose to reconstruct an image from the attenuation sinogram and use prior information in image space (e.g. known tissue attenuation in a certain region) to obtain the constant. To reconstruct the attenuation sinogram we use the MLTR algorithm [11]:

$$\mu_j^{(n+1)} = \mu_j^{(n)} + \frac{\sum_i l_{ij} \frac{\overline{y}_i - r_i}{\overline{y}_i} (\overline{y}_i - y_i)}{\sum_i l_{ij} \sum_k l_{ik} (\overline{y}_i - r_i)(1 - \frac{y_i r_i}{\overline{y}_i^2})} \quad (4)$$

where μ_j is the reconstructed attenuation value in voxel j, $\overline{y_i} = b_i \exp(-\sum_i l_{ij}\mu_j) + r_i$, l_{ij} is the intersection length of LOR i and pixel j. Equation 4 uses the measured activity $y_i = \sum_t y_{it}$ as transmission scan and the unattenuated forward projection of the reconstructed activity $b_i = \sum_{jt} c_{ijt}\lambda_j$ as the blank scan.

In order to determine the constant, agreement of some reconstructed attenuation values with the known attenuation coefficient of soft tissues at 511 keV was imposed [7, 12]. A region composed mostly of soft tissue was identified in the image and the mean attenuation coefficient in that region was computed. The region was determined by thresholding the central region of the image, keeping the values greater than the median over the region. Given the ratio of the correct tissue attenuation value to the extracted mean attenuation value (β), the following expression was used to estimate γ, the factor by which the activity image (and therefore the blank scan) had to be scaled.

$$\sum_i c_{ij}\gamma\lambda_j e^{-\mu\beta L} \simeq \sum_i c_{ij}\lambda_j e^{-\mu L} \rightarrow \gamma \simeq (e^{\mu L})^{\beta-1} \quad (5)$$

The blank scan was then rescaled with the factor γ, the attenuation image with β and a new MLTR-iteration was computed. This sequence of MLTR reconstruction and rescaling was repeated until $0.99 < \gamma < 1.01$, which typically happens after a few iterations. Note that the relation between the attenuation image and the transmission sinogram is nonlinear, which is why MLTR iterations are required to correctly propagate the effect of rescaling the activity with γ into the attenuation image.

3 Simulation experiments

In this section, the performance of a circular PET system for scanning a heart phantom is studied for different system parameters, including: full or limited angular coverage, sinogram truncation to a width W of 50 cm, a TOF resolution of 250 ps or 60 ps FWHM and presence or absence of a scatter contribution. The noise was modelled using 200 noise realizations with a moderate noise level of $8.5 \cdot 10^5$ counts in the activity sinogram. The 2D simulated randoms are scaled to obtain randoms to primary ratio of 50%.

The images were reconstructed with 20 iterations of the re-scaled MLACF algorithm outlined above, and post-smoothed with a 2D Gaussian with FWHM of 4 mm.

We analyze two types of systems. We will consider a limited angle system that we call "open configuration" (described in figure 1 left) and a "closed configuration" that is obtained by accepting all LORs seen by the panels if they were rotating continuously.

In order to challenge the reconstruction, four (three horizontal and one vertical) small Defrise phantoms were added to the heart phantom (see figure 1). These phantoms have been added with, from top to bottom, distances of 16, 10, 10 and 30 mm between the rods.

In the right part of figure 1 we compare the activity reconstructions for both re-scaled MLACF and MLEM with perfect attenuation map for the 250 ps in the case of limited angle for open and closed configuration

Figure 1 show that the performance of the re-scaled MLACF algorithm is close to the MLEM with perfect attenuation map as the difference between their values is low compared to the background activity.

For a scatter simulation study (figure **??**), a scatter sinogram was generated. It was produced by convolving the trues sinogram with a 3D Gaussian with a FWHM of 120 mm in radial direction, 0.43 radians in angular direction and 94 mm in TOF direction. After smoothing, the scatter sinogram was multiplied with a scatter to trues ratio of 70%. In the final sinogram, the ratio of scatters to prompts was 0.38. No scatter correction was applied to the reconstructed images.

The two narrowest horizontal Defrise phantoms are poorly reconstructed in the open configuration, but this is solved if the TOF resolution is improved to 60 ps (9 mm). As expected, the vertical Defrise phantoms are in any case well reconstructed. The absolute differences between the reconstructions and ground truth images (also post-smoothed with a 4 mm gaussian) are small.

4 Discussion

In this work, joint reconstructions of the activity and attenuation were done using a re-scaled MLACF approach. The scale factor can be determined by imposing a-priori known attenuation values to regions in the attenuation image [12]. When the scale factor is obtained, the activity image can be re-scaled accordingly, no new activity reconstruction is required. For these 2D simulations, a good value of the scale factor could be obtained, despite the presence of limited angle

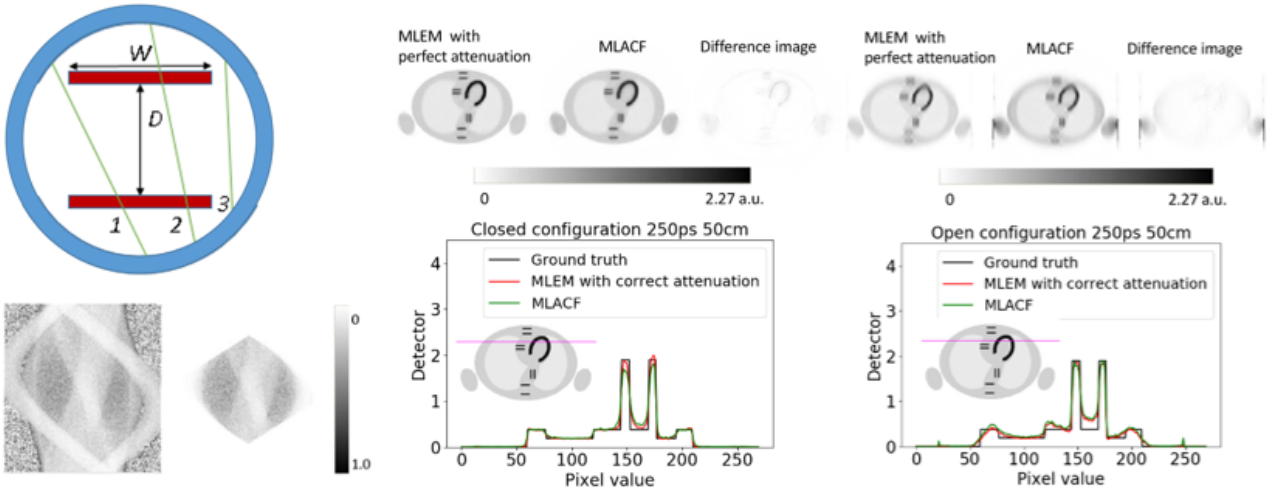

Figure 1: *Left up and down*: Description of the system and estimated attenuation sinograms for the closed and open configuration. *Up right*: Activity reconstructed images from perfect attenuation MLEM, re-scaled MLACF, and the difference image for closed and open configuration and 250 ps, respectively.*Bottom right*: Activity profiles along the line shown in the picture above. Even for the closed systems, the arms are outside the FOV and therefore not seen in all parallel projections.

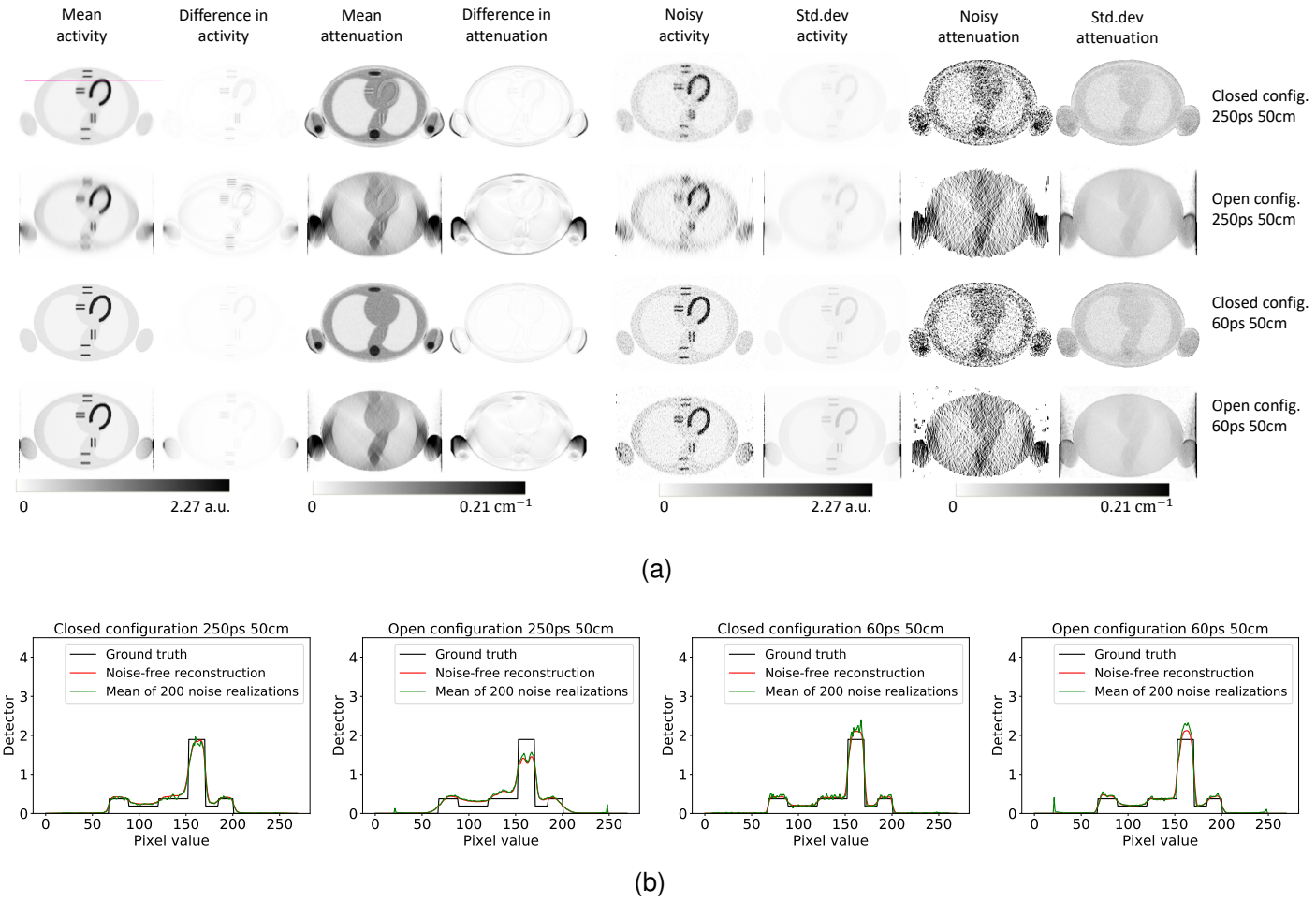

Figure 2: Results from 200 noise realisations for $W = 50$ cm without scatter contribution, (*from top to bottom):* closed configuration with 250 ps, open configuration with 250 ps, closed configuration with 60 ps and open configuration with 60 ps. In (a) and (*from left to right):* mean of the 200 noise realizations for the activity reconstruction, difference of this mean image with the ground truth, mean attenuation reconstruction, difference of this mean image with the ground truth, first noise realization of the activity, standard deviation for the 200 noise realizations of the activity, first noise realization of the attenuation and standard deviation of the attenuation. In (b) the line profiles of the activity image along a row through the apex of the heart (shown in (a) in purple) of the ground truth (black), the mean of 200 noise realizations (green) and the noiseless reconstructed image (red) for (*from left to right*) 250 ps closed configuration, 250 ps open configuration, 60 ps closed configuration and 60 ps open configuration.

artefacts.

In general, the images are worse for the open system, because of the increased amounts of missing data. For the closed system, the truncation is very limited, only part of the arms extend beyond the field of view and nearly artefact-free reconstructions are obtained. For the open system, the images are reconstructed from limited angle data. The horizontal Defrise phantoms, and in particular the two narrow ones, are poorly reconstructed when the TOF resolution is 250 ps, because the system has no projection data that "have seen" that there is a cold region between the hot rods. The vertical Defrise phantom is reconstructed accurately, because the two rods appear well separated in the acquired vertical projections. When the TOF resolution is improved to 60 ps, it provides a spatial resolution of 9 mm along the LORs. This enables the system to detect the cold region between the rods and to obtain accurate reconstruction of the Defrise phantoms.

Strong limited angle artifacts appeared in the attenuation and activity images near the edges of the phantom. MLACF is less performant if the activity is distributed along the LOR over a distance which is small compared to the TOF resolution. This is the case near the edges of the object. They produce an overestimation of the attenuation and activity estimates, which will adversely affect scatter estimates computed from the images, which, in turn, will propagate into the scatter corrected image. These effects will degrade image quality mostly near the edges of the object, but it can affect the central part to some extent. In addition, for the open system, the central part of the attenuation map is vertically blurred as a result of the missing data. Therefore, to ensure artefact-free and quantitative reconstruction of the activity near the center of the field of view, additional constraining of the attenuation image may be necessary, e.g. by imposing a maximum value to attenuation coefficients.

The analysis of the scatter estimation and correction problem is left for future research, but as a first exploration, the effect of a scatter estimation error on the performance of the re-scaled MLACF algorithm was investigated. For that purpose, re-scaled MLACF reconstructions without scatter correction were computed from scatter-contaminated sinograms. The reconstructed images are not exact, but they have a reasonably good visual quality. Based on these results, an iterative procedure alternating the estimation of the joint activity together with attenuation estimation and scatter estimation may work, even when initialized with a zero scatter estimate. We will evaluate this for fully 3D TOF-PET.

5 Conclusion

In this work, we investigated with simple 2D noise-free and noisy simulations the feasibility of obtaining attenuation corrected images from stand-alone limited angle TOF-PET systems. For the joint estimation of the activity and attenuation images, we proposed a re-scaled MLACF algorithm. We consider the results promising, warranting further investigation with more sophisticated fully 3D simulations and real PET measurements.

References

[1] A. J. González, F. Sánchez, and J. M. Benlloch. “Organ-dedicated molecular imaging systems”. *IEEE Transactions on Radiation and Plasma Medical Sciences* 2.5 (2018), pp. 388–403.

[2] P. Gravel, Y. Li, and S. Matej. “Effects of TOF resolution models on edge artifacts in PET reconstruction from limited-angle data”. *IEEE Transactions on Radiation and Plasma Medical Sciences* 4.5 (2020), pp. 603–612.

[3] Y. Li, M. Defrise, S. Matej, et al. “Fourier rebinning and consistency equations for Time-of-Flight PET planograms”. *Inverse Problems* 32 (Sept. 2016), p. 095004.

[4] M. Defrise, A. Rezaei, and J. Nuyts. “Time-of-Flight PET data determine the attenuation sinogram up to a constant”. *Physics in Medicine and Biology* 57 (Feb. 2012), pp. 885–99.

[5] A. Rezaei, M. Defrise, G. Bal, et al. “Simultaneous reconstruction of activity and attenuation in Time-of-Flight PET”. *IEEE Transactions on Medical Imaging* 31 (Aug. 2012), pp. 2224–33.

[6] S. Ahn, H. Qian, and R. Manjeshwar. “Convergent iterative algorithms for joint reconstruction of activity and attenuation from Time-of-Flight PET data”. *IEEE Nuclear Science Symposium Conference Record* (Oct. 2012), pp. 3695–3700.

[7] S. Ahn, L. Cheng, D. Shanbhag, et al. “Joint estimation of activity and attenuation for PET using pragmatic MR-based prior: Application to clinical TOF PET/MR whole-body data for FDG and non-FDG tracers”. *Physics in Medicine and Biology* 63 (Jan. 2018), p. 045006.

[8] A. Mehranian and H. Zaidi. “Joint estimation of activity and attenuation in whole-body TOF-PET/MRI using constrained gaussian mixture models”. *IEEE Transactions on Medical Imaging* 34 (Mar. 2015), pp. 1808–21.

[9] A. Rezaei, M. Defrise, and J. Nuyts. “ML-Reconstruction for TOF-PET with simultaneous estimation of the attenuation factors”. *IEEE Transactions on Medical Imaging* 33 (Apr. 2014), pp. 1563–72.

[10] M. Vergara, A. Rezaei, G. Schramm, et al. “2D feasibility study of joint reconstruction of attenuation and activity in limited angle TOF-PET”. *IEEE Transactions on Radiation and Plasma Medical Sciences* (Under review).

[11] K. Slambrouck and J. Nuyts. “Metal artifact reduction in computed tomography using local models in an image block-iterative scheme”. *Medical Physics* 39 (Nov. 2012), pp. 7080–93.

[12] Y. Li, S. Matej, and J. Karp. “Practical joint reconstruction of activity and attenuation with autonomous scaling for Time-of-Flight PET”. *Physics in Medicine and Biology* (Apr. 2020).